https://doi.org/10.48048/tis.2023.6384

Fine-Tuning the Degree of Negative Charge and Carboxylate Grafting Density of Polymer-Coated Magnetite Nanoparticle

Usana Mahanitipong, Patcharin Kanhakeaw and Metha Rutnakornpituk*

Department of Chemistry and Center of Excellence in Biomaterials, Faculty of Science, Naresuan University, Phitsanulok 65000, Thailand

(*Corresponding author's e-mail: methar@nu.ac.th)

Received: 23 November 2022, Revised: 29 December 2022, Accepted: 3 January 2023, Published: 5 January 2023

Abstract

The surface of magnetite nanoparticle (MNP) was modified with poly(acrylic acid)(PAA)-poly(ethylene glycol) methyl methacrylate (PEGMA) (co)polymer to obtain water dispersible MNP with pH sensitive surfaces *via* atom transfer radical polymerization (ATRP) of *tert*-butyl acrylate (*t*-BA), followed by the *t*-BA group deprotection. Molar compositions of the (co)polymer were systematically varied, namely 100:0, 75:25, 50:50 and 25:75 of P(*t*-BA)/PEGMA, respectively, such that the grafting density of carboxylate groups on the MNP surface after the deprotection can be fine-tuned. Transmission electron microscopy (TEM) indicated that the MNP were spherical (*ca*.5-12 nm in diameter) with some nanoclustering observed. The roles of PAA and PEGMA affecting the hydrodynamic size and zeta potential of the nanocomposites observed *via* photocorrelation spectroscopy (PCS) were discussed. The percentages of the polymeric composition in the nanocomposites in each step of the reaction were determined *via* thermogravimetric analysis (TGA) and their magnetic properties were studied *via* vibrating sample magnetometry (VSM). These novel nanocomposites with pH sensitive surface and magnetically guidable properties might be advantageous for further conjugations either by covalent or ionic bonding with bioentities.

Keywords: Nanoparticle, Magnetite, ATRP, Polyelectrolyte, PAA, PEGMA, pH Responsive

Introduction

The study in magnetite nanoparticle (MNP, Fe_3O_4) has gained a great attention in last few decades owing to its potential uses in various applications, e.g. protein and enzyme immobilization, separation and purification of bioentities (DNA, RNA, cells), enhancing agents in magnetic resonance imaging (MRI) and controlled drug release and delivery [1]. However, the undesirable aggregation of these particles owing to attractive interactions, including van der Waals, magnetic and gravitational forces, can limit its potential uses. Surface modification of MNP with long chain polymers has been markedly studied over the past decade to overcome this limitation [2,3]. The polymers coating on the MNP also provided the surface functionality, which was a key for controlling the particle's interaction with bioentities and improving its stability and dispersibility in its media [4]. Many approaches have been proposed in the preparation of polymer-coated MNP, e.g. physical and chemical adsorption [5], in-situ particle coprecipitation in the presence of polymers [6] and covalent bonding *via* silane chemistry [7,8].

The MNP coated with ionizable polymers, the so-called polyelectrolytes, has attracted great attentions recently [9,10]. In polar solvents such as water, their ionizable groups can dissociate, resulting in the formation of charges on the polymer chains and the release of counterions in solution. Examples of polyelectrolytes include polystyrene sulfonate [2], polyacrylic acid (PAA) [11], and polymethacrylic acids [12], and their salts, DNA and other polyacids and polybases [13]. In particular, the study in MNP surface modification with PAA has been much reported recently [14-16]. The carboxyl groups in PAA chains provided many advantages for the MNP, including 1) covalent coupling sites with other biomolecules, 2) providing steric and electrostatic repulsions, which essentially enhanced the particle stability and dispersibility, and 3) pH-responsive properties. Previous works reported the coating of MNP with PAA either *via* either "grafting-to" [17,18] or "grafting-from" approaches [19]. Atom transfer radical polymerization (ATRP), a kind of controlled radical polymerization, has markedly been of great interest for MNP surface modification because it does not require stringent experiment condition. In addition, it can be effectively used for synthesis of block and random copolymers with a wide range of monomers in a controllable fashion with narrow molecular weight distribution [19]. Many precedents have reported the

synthesis of well-defined PAA *via* ATRP by using acrylic acid monomer [20] or *tert*-butylacrylate monomer, followed by hydrolysis of the *tert*-butyl ester protective groups to essentially obtain PAA [21,22]. Interestingly, the copolymers of PAA and poly(ethylene glycol) (PEG) coated on MNP surface has also been reported [23,24]. Coating PEG on MNP can create a comb-type protecting layer to the particle to provide biocompatibility, dispersibility and diminish protein adsorption [18]. Hence, MNP coated with PAA-PEG copolymer showed many promising applications including anticancer drug delivery [22], and MRI diagnosis [24]. However, the study in fine-tuning the degree of negatively charged polymer by systematically varying the ratio of PAA to PEG components on MNP surface has never been reported.

In this work, surface modification of MNP with PAA/poly(ethylene glycol) methyl ether methacrylate (PEGMA) (co)polymer (100/0, 75/25, 50/50 and 25/75, respectively) *via* ATRP using a "grafting from" technique was studied. Due to the neutral nature of PEGMA and negative charge of PAA, the surface charge of the particles should be adjusted by varying the molar ratio of P(*t*-BA) to PEGMA in the surface modification *via* ATRP, followed by hydrolysis to gain PAA/PEGMA-coated MNP. MNP with tunable degrees of negative charge can be greatly advantageous in many applications. For example, it can be used to separate specific proteins *via* ion exchange and to covalently bind a variety of biomolecules [22,24,25]. In this work, the surface-initiated ATRP of P(*t*-BA)/PEGMA (co)polymer mediated by a copper complex was first carried out and the detail of this part has been previously reported [26]. The *t*-butyl groups on the particle surface were then deprotected to obtain the carboxylate groups on its surface [27,28]. The particle size of the (co)polymer-MNP nanocomposites were evidenced *via* transmission electron microscopy (TEM) and their magnetic property was elucidated *via* vibrating sample magnetometry (VSM). The hydrodynamic diameter and zeta potential values of the nanocomposite were measured *via* photocorrelation spectroscopy (PCS). In addition, quantitative analysis of the carboxylate groups presenting in the nanocomposites were also acquired from conductometric titration.

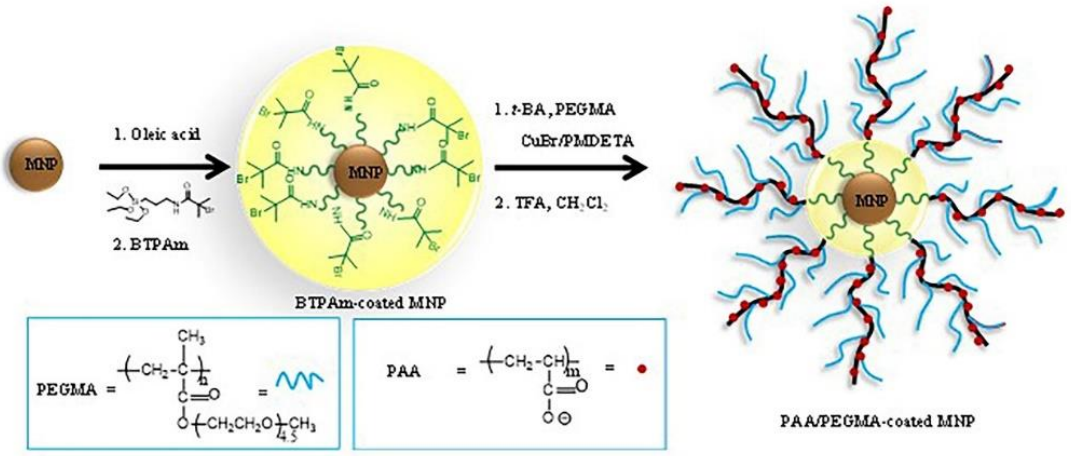

Figure 1 Synthesis scheme for PAA/PEGMA-coated MNP.

Materials and methods

Materials

The following reagents were used as received; iron (III) acetylacetonate ($Fe(acac)_3$), 99 %, (Acros), oleic acid (Fluka), 2-bromoisobutylryl bromide (BIBB), 98 %, (Acros), ethyl-2-bromoisobutyrate (EBIB), 98 %, (Aldrich), 3-aminopropyl triethoxysilane (APS), 99 %, (Acros), benzyl alcohol 98 %, (Unilab), triethylamine (TEA), 97 %, (Carto Erba), *N*,*N*,*N'*,*N''*,*N''*-pentamethylene triamine (PMDETA), 99 + %, (Acros), cupper(I) bromide (CuBr), 99.99 %, (Aldrich) and trifluoroacetic acid (TFA), 99 %, (Acros). *Tert*-butyl acrylate (*t*-BA, 99 % stabilized) (Acros) was dried in CaH_2 and distilled before use. Poly(ethylene glycol)methyl methacrylate (PEGMA, $\overline{M}_n$ = 300 g/mol) (Aldrich) was stored at −4 °C. 2-Bromo-2-methyl-*N*-(3-(triethoxysilyl)propyl)propanamide (BTPAm) were prepared as detailed in the previous report [19]. Toluene, dichloromethane (CH_2Cl_2), *N*,*N*-dimethyl formamide (DMF) (Unilab) and 1,4- dioxane (Unilab) were used after distillation over CaH_2.

Characterization

FTIR was performed on a Nicolet Avatar 370 DTGS spectrometer in the attenuated total reflection (ATR) mode. TEM were performed on a Philips Tecnai 12 operated at 120 kV equipped with Gatan model 782 CCD camera. Magnetic properties of the particles were performed on a Standard 7,403 Series, Lakeshore VSM and measured over a range of ± 10,000 G of applied magnetic fields. Thermogravimetric analysis (TGA) was measured on SDTA 851 Mettler-Toledo at the temperature range of 25 - 600 °C under O_2 atmosphere. PCS was carried out using NanoZS4700 nanoseries Malvern instrument. The sample dispersions were sonicated before each measurement without filtration. Determination of the number of carboxylate groups grafted on MNP was performed on Seveneasy conductometer (Metter Toledo Bmblt 8603 Swchwerzenbach). 1.50 mg of the (co)polymer-coated MNP was dispersed in 5 mL of a 0.005 M NaOH solution with stirring. The aqueous dispersion was then titrated with 0.005 M HCl solution.

Syntheses

Synthesis of BTPAm-immobilized MNP

$Fe(acac)_3$ (0.5 g, 1.41 mmol) was dissolved in benzyl alcohol (90 mL) and magnetically stirred at 180 °C for 48 h with nitrogen flow [26]. The particle was magnetically separated, washed with ethanol and CH_2Cl_2 and then dried *in vacuo*. After ultrasonication of the MNP dispersion (0.08 g of the MNP in 3 mL of toluene) for 1 h, oleic acid (0.4 mL) was added into the dispersion and then stirred for 3 h under N_2 atmosphere to obtain the oleic acid-immobilized MNP. BTPAm-immobilized MNP was synthesized *via* the reaction of the oleic acid-immobilized MNP (0.01 g), BTPAm (0.09 mL, 0.29 mmol) and 2 M TEA (0.05 mL) in toluene (1 mL). The mixture was magnetically stirred for 24 h under N_2 atmosphere, and the product was precipitated in methanol, washed with toluene, and dried *in vacuo*.

Synthesis of P(t-BA)/PEGMA-coated MNP

The MNP coated with P(*t*-BA)/PEGMA (co)polymers with various molar ratios of each composition (100/0, 75/25, 50/50, 25/75 molar ratios of *t*-BA/PEGMA, respectively) were prepared *via* ATRP using EBiB as a radical initiator. The reaction of 50/50 molar ratio of *t*-BA/PEGMA was herein described. BTPAm-immobilized MNP (0.2 g), *t*-BA (2.9 mL, 0.02 mol), PEGMA (5.7 mL, 0.02 mol) and EBiB (0.06 mL, 0.0004 mol) and 1,4-dioxane (5.0 mL, 60 %w/v) were mixed with ultrasonication for 15 min and then was degassed by 3 freeze-pump-thaw cycles. PMDETA (0.08 mL, 0.0004 mol), CuBr (0.06 g, 0.02 mol) and DMF (0.45 mL, 5 %v/v) were introduced to the solution under nitrogen atmosphere. The solution was heated to 90 °C with stirring. The (co)polymer-MNP nanocomposites were precipitated in diethyl ether. The nanocomposites were then magnetically separated and dried *in vacuo.*

Deprotection of t-butyl groups of P(t-BA) to obtain PAA/PEGMA-coated MNP

P(*t*-BA)/PEGMA-coated MNP (0.10 g) was resuspended in CH_2Cl_2 (20 mL) containing 0.5 M TFA (1.40 mL) and the mixture was continuously stirred for 24 h. The resulting PAA/PEGMA-coated MNP were gradually precipitated in CH_2Cl_2. The particles were washed with CH_2Cl_2, magnetically separated and dried *in vacuo*.

Determination of the number of carboxylate groups on the MNP surface

The number of carboxylate groups grafted on the surface of the (co)polymer-coated MNP was determined by conductometric titration and estimated from the following equation [29]:

$$[Carboxylate] = \frac{V \times M \times N_A}{SC} \quad (1)$$

where [carboxylate] = the number of carboxylate groups (molecules/g of the nanocomposite)
V = the used volume of HCl solution in region II (L)
M = the concentration of HCl used (mol/L)
N_A = the Avogadro's number
SC = the weight of the nanocomposite used (g)

In these experiments, the concentration of HCl solution was 0.005 mol/L and the weight of the nanocomposite was 1.50 mg.

Results and discussion

Deprotection of t-butyl groups of PAA/PEGMA (co)polymer coated on MNP surface

P(*t*-BA)/PEGMA-coated MNP (100/0, 75/25, 50/50 and 25/75 molar ratio) were then used for further studies in deprotection of *t*-butyl groups of P(*t*-BA) on the particle surface. After the deprotection, it was anticipated that PAA/PEGMA-coated MNP was gained. FTIR spectra in **Figure 2** show the functional groups of 50/50 P(*t*-BA)/PEGMA-coated MNP before the deprotection and PAA/PEGMA-coated MNP after the deprotection of all 4 (co)polymer compositions. It evidences the transformation from a sharp and strong peak of carbonyl groups of esters (1,728 cm^{-1}) to a broad and strong peak (1,690 cm^{-1}) of carboxylic acid functional groups. The shift of C-O bond stretching signals of esters (1,143 cm^{-1}) to those of carboxylic acid (1,203 cm^{-1}) was another evidence of the occurrence of the deprotection reaction. In addition, the depletion of the doublet signals (1,389 - 1,367 cm^{-1}) of C-H bending of *t*-butyl groups in combination with the presence of a broad and strong signal of N-H, O-H stretching (3,416 cm^{-1}) was another supportive result indicating the formation of PAA on the particle surface.

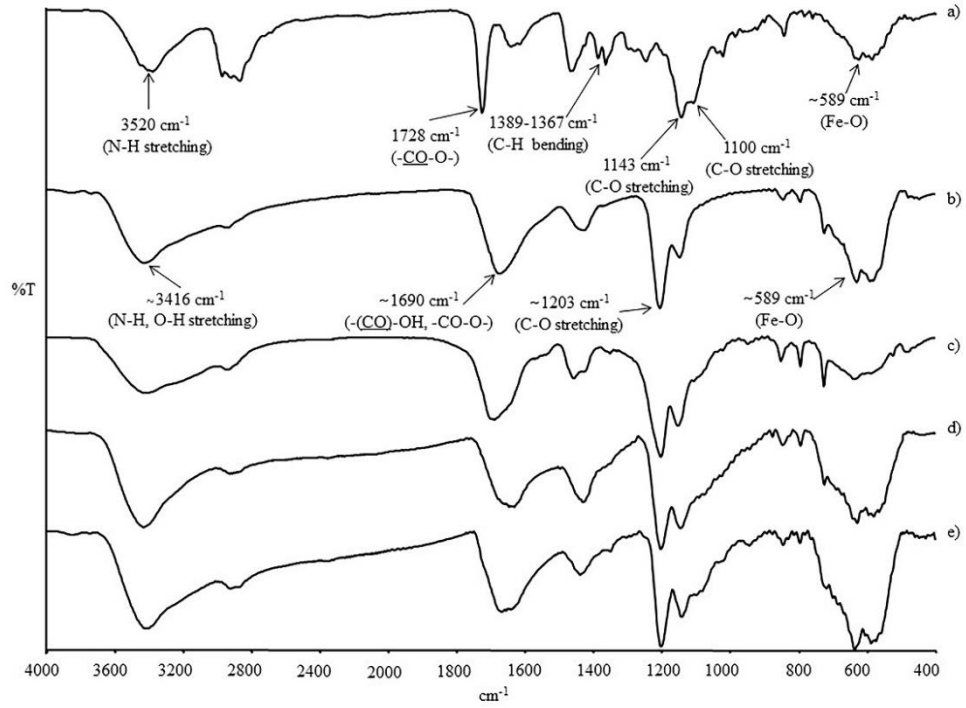

Figure 2 FTIR spectra of (a) 50/50 P(*t*-BA)/PEGMA-coated MNPs (before deprotection) and PAA/PEGMA-coated MNP (after deprotection) having molar ratio of PAA/PEGMA of (b) 100/0, (c) 75/25, (d) 50/50, and (e) 25/75, respectively.

TEM images and the particle size distribution of P(*t*-BA)-, PAA-, and PAA/PEGMA-coated MNP were exhibited in **Figure 3**. The particle size ranged between 5 to 12 nm with the average of *ca*.8 nm. It should be noted that P(*t*-BA)-coated MNP were well dispersed in toluene due to the presence of hydrophobic P(*t*-BA) coating on the particle surface (**Figure 3(a)**), while PAA-coated MNPs were well dispersed in water because of the presence of hydrophilic and charge surfactants of PAA (**Figure 3(b)**). Interestingly, the introduction of PEGMA on the particle surface seemed to induce the formation of nanoclustering as shown in **Figure 3(c)** and this was attributed to the decrease of negatively charged PAA in the copolymer. The degree of nanoclustering of the particles seemed to increase when decreasing the percentage of PAA in the copolymer (**Figure 3(d)**). The polymer layers can be apparently observed when there were some nanoclusters formed as labeled in **Figures 3(c) - 3(d)**.

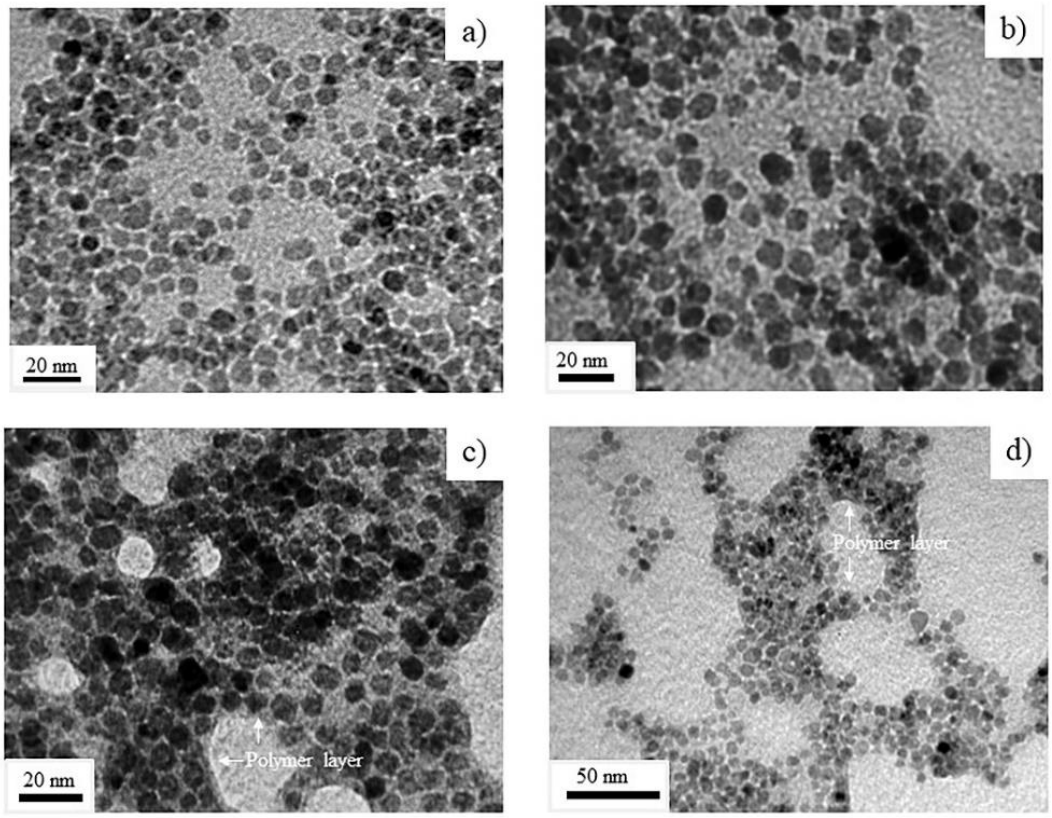

Figure 3 TEM images of (a) P(*t*-BA)-coated MNP (prepared from toluene dispersion), (b) PAA-coated MNP, (c) 75/25 PAA/PEGMA-coated MNP, and (d) 50/50 PAA/PEGMA-coated MNP (prepared from aqueous dispersions).

Zeta potential and hydrodynamic diameter of PAA-coated MNP and PAA/PEGMA-coated MNP were determined as a function of pH of aqueous solutions *via* photocorrelation spectroscopy (PCS). It is known that carboxylic acid functional groups of PAA can be ionized and essentially form carboxylate anions in alkaline solutions. The effect of the pH change on hydrodynamic size and degree of the surface charges of the polymer-coated MNP attracted our attention.

In PAA-coated MNP (**Figure 4(a)**), their hydrodynamic diameter gradually decreased in the range of acidic pH (pH 1 - 5) and rapidly decreased as the dispersion pH was continuously increased up to 11. It was rationalized that ionization of carboxylate groups on the particle surface took place in basic pH (**Figure 5(a)**). These carboxylate anions gave rise to additional electrostatic repulsion and essentially inhibited the formation of large aggregates [30-33].

In the case of PAA/PEGMA copolymer-coated MNP (**Figures 4(b) - 4(d)**), the pH dependence of the dispersions on zeta potential showed similar behavior to the case of PAA-coated MNP; their surface charges became more negative as increasing pH of the dispersions. Their surface charges ranged between +40 and −50 mV. Electrostatic stabilization of the nanocomposites was apparently enhanced in the range of high acidic or basic pH due to the repulsion of the same charges of the polymers coating on the particle surface, resulting in the promotion of the particle dispersibility in water and essentially formed the particles with relatively small hydrodynamic size (**Figure 5(b)**). Interestingly, the hydrodynamic diameter of the copolymer-coated MNP drastically increased up to about 1 μm (~1,100 - 1,400 nm) at pH between 5 and 7 (**Figures 4(b) - 4(d)**). This was probably due to the presence of PEGMA on their surface, resulting in the formation of entanglement of the dangling brush of PEGMA which might overcome the electrostatic repulsion at the pH close to the point of zero charge (PZC) of the nanocomposites. It should be noted that this phenomenon was not observed in the PAA-coated MNP (**Figure 4(a)**). TEM experiments also showed a supportive result to this proposed mechanism as indicated by the presence of some nanoclustering of multiple nanoparticles (**Figure 3(d)**). This nanoclustering was not observed in the TEM image of PAA-coated MNP (**Figure 3(b)**).

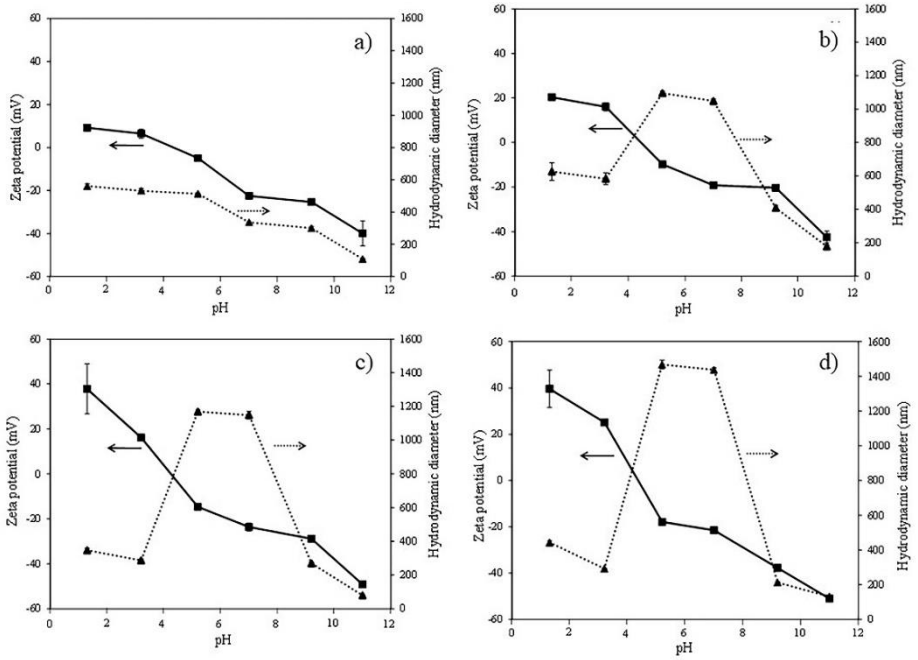

Figure 4 Effect of the pH change on zeta potential and hydrodynamic diameter of the particles. PAA/PEGMA molar ratios in PAA/PEGMA-coated MNP were (a) 100/0, (b) 75/25, (c) 50/50, and (d) 25/75, respectively.

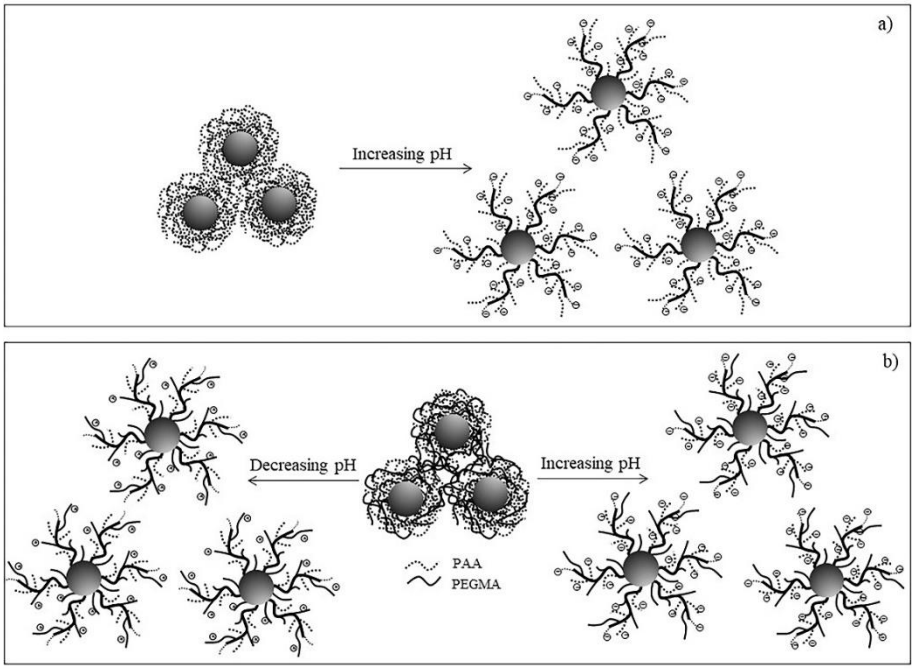

Figure 5 The proposed mechanisms of the electrostatic repulsion of (a) PAA-coated MNP in basic pH and (b) PAA/PEGMA-coated MNPs in acidic and basic pH.

Percentages of the polymer in the composites in each step of the reactions (bare MNP, BTPAm-coated MNP, P(t-BA)/PEGMA-coated MNP and PAA/PEGMA MNP) were determined *via* TGA technique. Examples of the TGA thermograms in the case of 50/50 PAA/PEGMA MNP are shown in **Figure 6**. It was assumed that the remaining weight (% char yield) was the weight of Fe and Si completely oxidized, and the loss weight was those of organic components including the polymer. The TGA thermogram of bare MNP (**Figure 6(a)**) shows the weight loss of 12 % upon heating to 600 °C and this was most likely due to

the residual benzyl alcohol remaining in the particle. When taking the loss weight of bare MNP into account, the organic component of BTPAm-coated was 7 wt% (**Figure 6(b)**) and those of P(*t*-BA)/PEGMA-coated MNP was 36 wt% (**Figure 6(d)**). After the deprotection step, the percentage of the organic components in PAA/PEGMA-coated MNP (**Figure 6(c)**) was 21 wt% and this number was significantly lower as compared to those of P(*t*-BA)/PEGMA-coated MNP (36 wt%) due to the removal of *t*-butyl groups from the polymeric layer of the particle [19,34]. Percentages of each component in the nanocomposites and their precursors are shown in Supporting information.

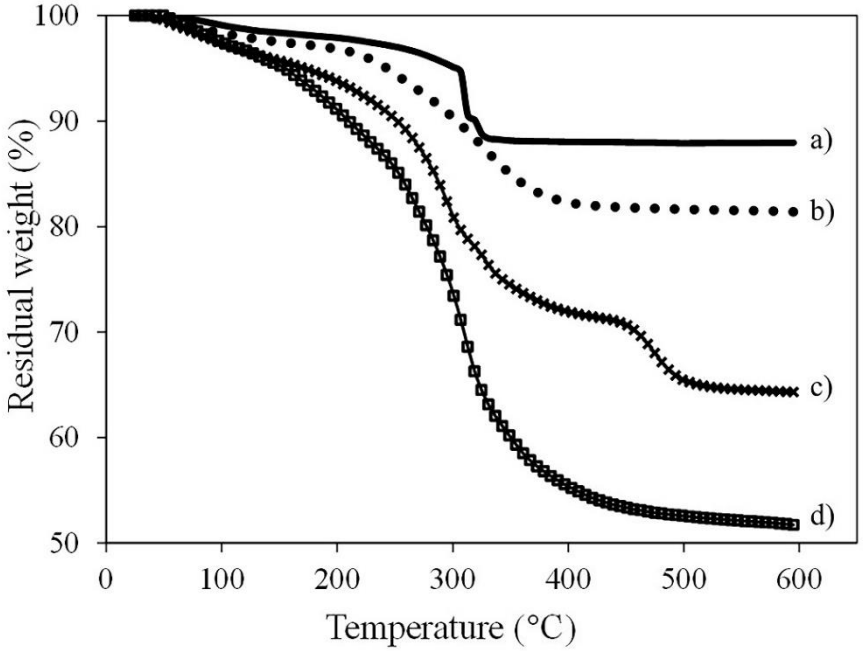

Figure 6 TGA thermograms of (a) bare MNP, (b) BTPAm-coated MNP and (c) 50/50 PAA/PEGMA-coated MNP, and (d) 50/50 P(*t*-BA)/PEGMA-coated MNP.

Hysteresis curves of bare MNP, BTPAm-coated MNP and PAA/PEGMA-coated MNP having various PAA/PEGMA ratios were exhibited in **Figure 7**. The particles showed superparamagnetic behavior at room temperature as indicated by the absence of magnetic remanence (M_r) and coercitivity (H_c). Bare MNP showed high saturation magnetization (M_s) (56 emu/g) (**Figure 7(a)**), while BTPAm-coated MNP showed a slight decrease in the M_s value (52 emu/g) due to the presence of a thin layer of BTPAm on MNP surface (**Figure 7(b)**). Similarly, the M_s values of PAA/PEGMA-coated MNP were significantly lower than that of the bare MNP, which was again probably due to the presence of non-magnetic polymer coated in the nanocomposites [19]. The M_s values of PAA/PEGMA-coated MNPs having various PAA/PEGMA ratios and their precursors are shown in Supporting information.

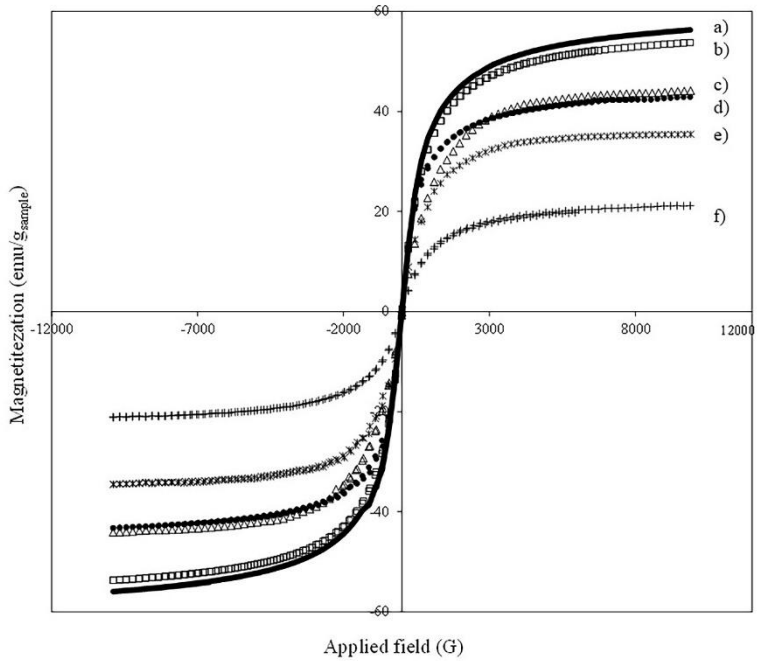

Figure 7 Magnetization curves of (a) bare MNP, (b) BTPAm-coated MNP, PAA/PEGMA-coated MNP having (c) 100/0, d) 75/25, (e) 50/50, and (f) 25/75, respectively.

Determination of the numbers of carboxylate groups on the MNP surface

Figure 8(a) illustrates the titration curve of the reaction between HCl and NaOH in the presence of 50/50 PAA/PEGMA-coated MNP. In this experiment, the carboxylate groups on the MNP surface were first exposed in excess NaOH solution. The reaction taking place was following [35]:

$$-COO^- + H^+ \xrightarrow{Na^+ \quad OH^-} -COO^- + Na^+ + H_2O + Na^+OH^-_{excess} \tag{2}$$

In region I, because of the strong basicity of excess OH^- in the solution as compared to that of $–COO^–$, the $OH^–$ anion in the mixture was predominantly neutralized once HCl was titrated.

$$Na^+_{excess} + OH^-_{excess} \xrightarrow{H^+ \quad Cl^-} H_2O + Na^+ + Cl^- \tag{3}$$

In region II, when the $OH^–$ ions in the solution were completely neutralized, the titrated H^+ ions then reacted with the $–COO^–$ groups on the surface of MNP. Once these $–COO^–$ groups were completely reacted, the solution conductivity abruptly increased owing to the excess of H^+ and Na^+ ions remaining.

Figure 8(b) exhibits the grafting density of carboxylate groups on (co) polymer-coated MNP surface. The grafting density of carboxylate groups consistently increased from 6.8×10^{21} to 8.8×10^{21} carboxylates/g of the nanocomposite as the molar ratio of PAA in the (co) polymers increased from 25 to 100. The example of the calculation is shown in Supporting information.

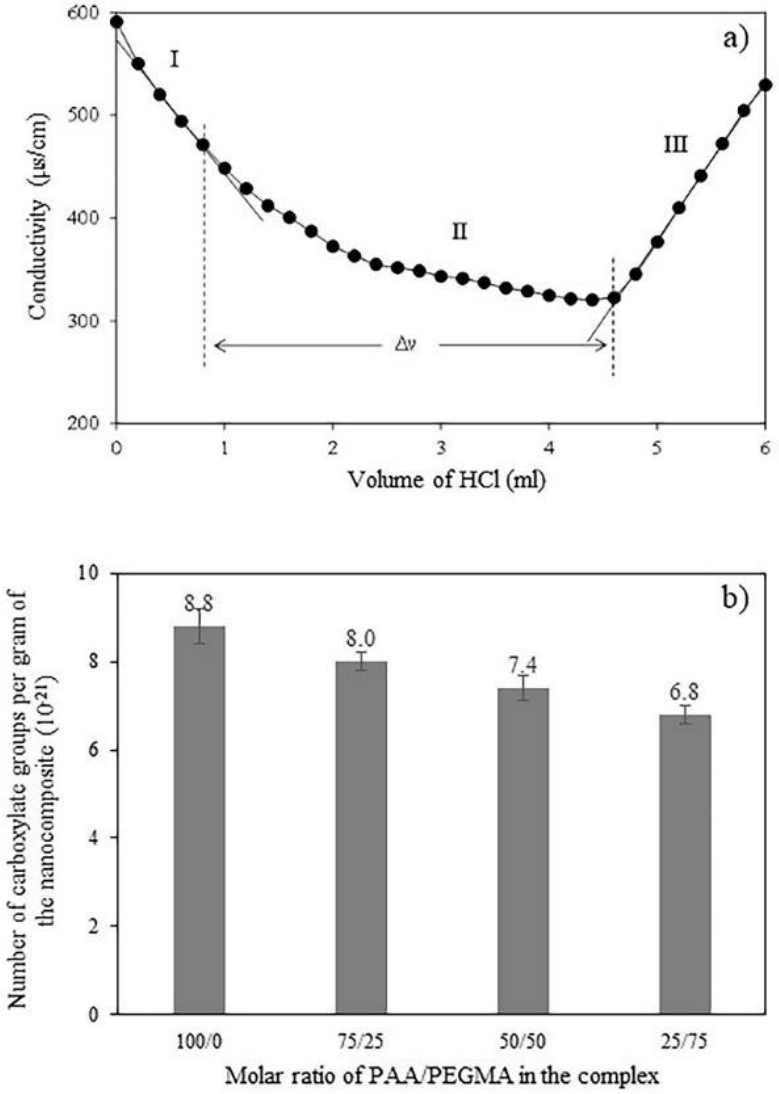

Figure 8 (a) The titration curve of the reaction between NaOH and HCl in the presence of 50/50 PAA/PEGMA-coated MNP and (b) the grafting density of the carboxylate groups on the MNP surface coated with PAA/PEGMA copolymers having various PAA/PEGMA ratios.

Conclusions

The degree of negatively charged polymer on MNP surface was fine-tuned by varying the ratio of *t*-BA to PEGMA used in the copolymerization via a "grating-from" surface-initiated ATRP, followed by the deprotection reaction. In PAA-coated MNP, increasing the solution pH resulted in the increase in negative charge of the particles and the decrease in its hydrodynamic size. In PAA/PEGMA-coated MNP, the presence of PEGMA increased the hydrodynamic size of the nanocomposites probably due to the interparticle entanglement. The presence of hydrophilic PAA and PEGMA on MNP surface not only promoted the particle dispersibility in water, but the presence of the carboxylate groups in the polymer structure also provided a platform for further functionalization with biomolecules of interest. These magnetically guidable nanocomposites with tunable density of carboxylate groups might be applicable for use as capturing supports with positively charged bioentities or as an intermediate for covalent coupling with biomolecules containing affinity functional groups.

Acknowledgements

This work was financially supported by National Research Council of Thailand (NRCT) (R2566B030). UM acknowledges the Science Achievement Scholarship of Thailand (SAST) for the scholarship.

References

[1] T Theppaleak, B Rutnakornpituk, U Wichai, T Vilaivan and M Rutnakornpituk. Magnetite nanoparticle with positively charged surface for immobilization of peptide nucleic acid and deoxyribonucleic acid. *J. Biomed. Nanotechnology* 2013; **9**, 1509-20.

[2] BW Chen, YC He, SY Sung, TTH Le, CL Hsieh, JY Chen, ZH Wei and DJ Yao. Synthesis and characterization of magnetic nanoparticles coated with polystyrene sulfonic acid for biomedical applications. *Sci. Tech. Adv. Mater.* 2020; **21**, 471-81.

[3] X Guan, S Yan, Q Zeng, Z Xu, Y Chen and H Fan. Polyacrylic acid-grafted magnetite nanoparticles for remediation of Pb(II)-contained water. *Fibers Polymers* 2016; **17**, 1131-9.

[4] S Meerod, B Rutnakornpituk, U Wichai and M Rutnakornpituk. Hydrophilic magnetic nanoclusters with thermo-responsive properties and their drug controlled release. *J. Magnetism Magnetic Mater.* 2015; **392**, 83-90.

[5] N Deepuppha, A Thongsaw, B Rutnakornpituk, WC Chaiyasith and M Rutnakornpituk. Alginate-based magnetic nanosorbent immobilized with aptamer for selective and high adsorption of Hg^{2+} in water samples. *Environ. Sci. Pollut. Res.* 2020; **27**, 12030-8.

[6] N Deepuppha, S Khadsai, B Rutnakornpituk, F Kielar and M Rutnakornpituk. Reusable pectin-coated magnetic nanosorbent functionalized with an aptamer for highly selective Hg^{2+} detection. *Polym. Adv. Technol.* 2021; **32**, 2207-17.

[7] B Thong-On, B Rutnakornpituk, U Wichai and M Rutnakornpituk. Magnetite nanoparticle coated with amphiphilic bilayer surfactant of polysiloxane and poly (poly (ethylene glycol) methacrylate). *J. Nanoparticle Res.* 2012; **14**, 953.

[8] U Mahanitipong and M Rutnakornpituk. Palladium-immobilized polymer-coated magnetic nanocomposites as reusable catalysts for the reduction of 4-nitrophenol. *Polym. Int.* 2022; **71**, 1119-26.

[9] S Stafford, C Garnier and YK Gun'ko. Polyelectrolyte-stabilised magnetic-plasmonic nanocomposites. *Nanomaterials* 2018; **8**, 1044.

[10] D Patiño-Ruiz, L Sanchez-Botero, J Hinestroza and A Herrera. Modification of cotton fibers with magnetite and magnetic core-shell mesoporous silica nanoparticles. *Phys. Status Solidi Appl. Mater.* 2018; **215**, 1800266.

[11] D Chełminiak, M Ziegler-Borowska and H Kaczmarek. Synthesis of magnetite nanoparticles coated with poly(acrylic acid) by photopolymerization. *Mater. Lett.* 2016; **164**, 464-7.

[12] R Wang, J lin, SH Huang, QY Wang, Q Hu, S Peng, LN Wu and QH Zhou. Disulfide cross-linked poly(methacrylic acid) iron oxide nanoparticles for efficiently selective adsorption of Pb(II) from aqueous solutions. *ACS Omega* 2021; **6**, 976-87.

[13] AV Dobrynin and M Rubinstein. Theory of polyelectrolytes in solutions and at surfaces. *Prog. Polym. Sci.* 2005; **30**, 1049-118.

[14] Z Mozafari, B Massoumi and M Jaymand. A novel stimuli-responsive magnetite nanocomposite as de novo drug delivery system. *Polym. Plast. Technol. Mater.* 2019; **58**, 405-18.

[15] D Niu, X Liu, Y Li, Z Ma, W Dong, S Chang, W Zhao, J Gu, S Zhang and J Shi. Fabrication of uniform, biocompatible and multifunctional PCL-b-PAA copolymer-based hybrid micelles for magnetic resonance imaging. *J. Mater. Chem.* 2011; **21**, 13825-31.

[16] A Dolatkhah and LD Wilson. Magnetite/polymer brush nanocomposites with switchable uptake behavior toward methylene blue. *ACS Appl. Mater. Inter.* 2016; **8**, 5595-607.

[17] S Wan, Y Zheng, Y Liu, H Yan and K Liu. Fe_3O_4 nanoparticles coated with homopolymers of glycerol mono (meth) acrylate and their block copolymers. *J. Mater. Chem.* 2005; **15**, 3424-30.

[18] E Illés, E Tombácz, M Szekeres, IY Tóth, Á Szabó and B Iván. Novel carboxylated PEG-coating on magnetite nanoparticles designed for biomedical applications. *J. Magnetism Magnetic Mater.* 2015; **380**, 132-9.

[19] M Rutnakornpituk, N Puangsin, P Theamdee, B Rutnakornpituk and U Wichai. Poly (acrylic acid)-grafted magnetic nanoparticle for conjugation with folic acid. *Polymer* 2011; **52**, 987-95.

[20] H Derakhshankhah, B Haghshenas, M Eskandani, R Jahanban-Esfahlan, S Abbasi-Maleki and M Jaymand. Folate-conjugated thermal-and pH-responsive magnetic hydrogel as a drug delivery nano-

system for “smart” chemo/hyperthermia therapy of solid tumors. *Mater. Today Commun.* 2022; **30**, 103148.
[21] Á Szabó, I Szanka, G Tolnai, G Szark and B Iván. LCST-type thermoresponsive behaviour of interpolymer complexes of well-defined poly (poly(ethylene glycol) methacrylate)s and poly(acrylic acid) synthesized by ATRP. *Polymer* 2017; **111**, 61-6.
[22] M Guo, Y Yan, H Zhang, H Yan, Y Cao, K Liu, S Wan, J Huang and W Yue. Magnetic and pH-responsive nanocarriers with multilayer core-shell architecture for anticancer drug delivery. *J. Mater. Chem.* 2008; **18**, 5104-12.
[23] E Illés, M Szekeres, IY Tóth, Á Szabó, B Iván, R Turcu, L Vékás, I Zupkó, G Jaics and E Tombácz. Multifunctional PEG-carboxylate copolymer coated superparamagnetic iron oxide nanoparticles for biomedical application. *J. Magnetism Magnetic Mater.* 2018; **451**, 710-20.
[24] E Illés, M Szekeres, IY Tóth, K Farkas, I Földesi, Á Szabó, B Iván and E Tombácz. PEGylation of superparamagnetic iron oxide nanoparticles with self-organizing polyacrylate-PEG brushes for contrast enhancement in MRI diagnosis. *Nanomaterials* 2018; **8**, 776.
[25] M Guo, C Que, C Wang, X Liu, H Yan and K Liu. Multifunctional superparamagnetic nanocarriers with folate-mediated and pH-responsive targeting properties for anticancer drug delivery. *Biomaterials* 2011; **32**, 185-94.
[26] P Kanhakeaw, B Rutnakornpituk, U Wichai and M Rutnakornpituk. Surface-initiated atom transfer radical polymerization of magnetite nanoparticles with statistical poly(tert-butyl acrylate)-poly(poly (ethylene glycol) methyl ether methacrylate) Copolymers. *J. Nanomaterials* 2015; **2015**, 1-10.
[27] G Gratzl, C Paulik, S Hild, JP Guggenbichler and M Lackner. Antimicrobial activity of poly(acrylic acid) block copolymers. *Mater. Sci. Eng. C* 2014; **38**, 94-100.
[28] SD Sütekin and O Güven. Preparation of poly(tert-butyl acrylate)-poly(acrylic acid) amphiphilic copolymers *via* radiation-induced reversible addition-fragmentation chain transfer mediated polymerization of tert-butyl acrylate. *Polym. Int.* 2020; **69**, 693-701.
[29] A Musyanovych, R Rossmanith, C Tontsch and K Landfester. Effect of hydrophilic comonomer and surfactant type on the colloidal stability and size distribution of carboxyl-and amino-functionalized polystyrene particles prepared by miniemulsion polymerization. *Langmuir* 2007; **23**, 5367-76.
[30] S Berger, ASynytska, L Ionov, KJ Eichhorn and M Stamm. Stimuli-responsive bicomponent polymer janus particles by “grafting from”/“grafting to” approaches. *Macromolecules* 2008; **41**, 9669-76.
[31] K Chen, Y Zhu, Y Zhang, L Li, Y Lu and X Guo. Synthesis of magnetic spherical polyelectrolyte brushes. *Macromolecules* 2011; **44**, 632-9.
[32] J Hang, L Shi, X Feng and L Xiao. Electrostatic and electrosteric stabilization of aqueous suspensions of barite nanoparticles. *Pow. Technol.* 2009; **192**, 166-70.
[33] Z Sui, JA Jaber and JB Schlenoff. Polyelectrolyte complexes with pH-tunable solubility. *Macromolecules* 2006; **39**, 8145-52.
[34] H Kong, C Gao and D Yan. Constructing amphiphilic polymer brushes on the convex surfaces of multi-walled carbon nanotubes by in situ atom transfer radical polymerization. *J. Mater. Chem.* 2004; **14**, 1401-5.
[35] RD Braun. *Introduction to chemical analysis*. Britannica, Illinois, 1982.